Spatial estimation methods for mapping corn silage and grain yield monitor data

Jason B. Cho[1] · Joseph Guinness[2] · Tulsi P. Kharel[1] · S. Sunoj[1] · Dilip Kharel[1] ·
Erasmus K. Oware[3] · Jan van Aardt[4] · Quirine M. Ketterings[1]

Abstract

Harvester-mounted yield monitor systems are increasingly used to document corn (*Zea mays* L.) yield. The three most commonly used spatial estimation methods to convert point data gathered with yield monitors to regular, grid-based, raster maps include nearest neighbor (NN), inverse distance weighting (IDW) and kriging. Seven spatial estimation methods (NN, IDW using 10, 20, 30 and all data points and kriging with exponential and Matérn covariance functions) were evaluated to determine the method that most accurately captures intra-field spatial variability of corn silage and corn grain yield in New York. Yield monitor data from two dairy farms and two grain operations were cleaned using Yield Editor prior to spatial analyses. The dataset included 7–10 years of data per farm for a combined 7484 ha (245 fields) of silage and 6971 ha (253 fields) of grain. Data were split into training (80%) and cross-validation datasets (remaining 20% of the data). Normalized root mean squared error (NRMSE) was used to evaluate the accuracy of the spatial estimation methods. Kriging with the Matérn covariance function resulted in the most accurate corn silage and grain yield raster maps both at the farm and field level. There were statistically significant differences in NRMSE between kriging with the Matérn isotropic covariance function and all other models for both corn silage and grain, regardless of field size, year when data were obtained or farm that supplied the data. These results are beneficial to ensure accurate and precise spatial mapping of yield products toward optimized corn growth management.

Keywords Corn silage · Corn grain · Yield monitors · Yield mapping · Spatial estimation methods

✉ Quirine M. Ketterings
  qmk2@cornell.edu

[1]   Department of Animal Science, Cornell University, Ithaca, NY, USA

[2]   Department of Statistics and Data Science, Cornell University, Ithaca, NY, USA

[3]   Department of Geology, University at Buffalo, Buffalo, NY, USA

[4]   Chester F. Carlson Center for Imaging Science, Rochester Institute of Technology, Rochester, NY, USA

Abbreviations

CV	Coefficient of variation
EC	Electrical conductivity
GP	Gaussian process
GNSS	Global navigation satellite systems
IDW	Inverse distance weighting
NDVI	Normalized Difference Vegetation Index
NN	Nearest neighbor
NRMSE	Normalized root mean squared error
US	United States

Introduction

Corn is a major crop in New York, with more than 400 000 ha planted annually. In 2019, 220 000 ha (55%) were combined for grain, while 180 000 ha (45%) were harvested for corn silage (USDA 2019a). Corn silage, typically grown in rotation with hay, is especially important to the dairy industry in New York; the state is ranked third in dairy production in the United States, following California and Wisconsin, and fourth in corn silage production, following Wisconsin, California and Minnesota (USDA 2019b).

Being able to measure corn silage and grain yield at the field and within-field levels is important, as understanding yield and variability in yield over time allows for better inventory management, production optimization and improved allocation of limited resources, such as seed and fertilizer (Long et al. 2016). With greater accessibility and affordability of yield monitor systems, more corn producers are now gathering spatially explicit yield monitor data with flow and moisture sensors that record readings every second as the harvester travels through a field. The availability of spatial data over multiple years allows for analyses of both spatial and temporal variability of yield (Kharel et al. 2019a). Such knowledge can help build actionable insights to better manage nutrients and increase yield (Maestrini and Basso 2018a).

Raw yield monitor data cannot be used right away, however, because the data not only reflect systematic yield variation within a field, but also measurement errors associated with yield-mapping (Dobermann and Ping 2004; Vega et al. 2019). Kharel et al. (2019b) suggested that three main factors cause systematic measurement errors even when proper calibration procedures are implemented: (1) sensor delays, (2) velocity calibration and (3) human errors. Delays exist because the main sensors in yield monitor systems (flow rate sensors, moisture sensors and global navigation satellite systems [GNSS] units) are embedded at different locations on harvest equipment, which causes flow and moisture values to be out of sync with corresponding GNSS readings. Velocity calibrations also heavily affect the data, as harvest equipment is calibrated for a certain velocity range (Arslan and Colvin 2002). Theoretically, measurement errors from inadequate velocity calibrations can be reduced by driving the equipment with constant travel speed, but due to irregular field shapes and variation in elevation of many fields in New York, such practice is highly impractical. Human errors occur, among others, when the operator does not raise the harvester head after completion of a pass, in which case the pass number will not be updated in the dataset. This can cause overlapping passes and hence artificially low yield around field edges. Thus, post-harvest yield data correction

and cleaning algorithms need to be applied to reduce measurement errors (Arslan and Colvin 2002; Blackmore 1999; Kharel et al. 2018, 2019b).

Yield monitor datasets consist of irregularly placed point estimates of grain flow, moisture and yield estimates; such irregularities are caused by differences in field shape, size and harvest patterns within a field. Researchers often use a rasterized yield map based on yield monitor data as a base layer in delineating zones for better field and resource management (Basso et al. 2007; Blackmore 2000; Brock et al. 2005; Buttafuoco et al. 2017; Diker et al. 2004; Hornung et al. 2006; Kharel et al. 2019a; Khosla et al. 2008) or as a means to understand variability in yield with regards to soil type, elevation and other topographical information (Anderson-Cook et al. 2002; Cox and Gerrard 2007; Kitchen et al. 1999; Maestrini and Basso 2018a, b; Yang et al. 2001) (Table 1). Yield data are typically not collected at the same GNSS locations each year, but once point data are translated into raster maps using regular grid cells, temporal yield variation can be analyzed with multiple years of data (Kharel et al. 2019a). Independent of use, point data need to be translated into regular grids (raster maps) to generate yield maps for farmers, especially where point maps are irregular and gaps in yield data exist.

The three most common approaches to developing raster maps from point data include nearest neighbor (NN), inverse distance weighting (IDW) with varying number of nearest points and kriging (Table 1; Ross et al. 2008). As the name suggests, NN uses the yield value of the nearest observation to estimate yield while IDW uses a weighted average of nearest neighbors, with weights proportional to the inverse distance. Assuming that there are n set of co-ordinates, $z_1, z_2, \ldots, z_n$ and their yield values, denoted as $Y(z_i)$ for $i \in \{1, \ldots, n\}$, at those co-ordinates, to estimate yield at co-ordinates x where the yield value is not known, the estimated yield value at location x, denoted as $Y(x)$ can be calculated as follows:

$$\overline{Y}(x) = \frac{\sum_{i=1}^{n} \frac{Y(z_i)}{d(z_i,x)^n}}{\sum_{i=1}^{n} \frac{1}{d(z_i,x)^n}} \tag{1}$$

where $d(z_i, x)$ represents distance between co-ordinates z_i and x and n is some natural number. In this case, n was set to 1. By weighting sample observations by the inverse of distance, observations that are closer to the estimated location will have higher weights than the observations that are further away. Kriging, also known as Gaussian Process (GP) regression, models spatial correlation between sample points. Spatial correlation can be modeled using various covariance functions. The Matérn and exponential functions, two commonly used covariance functions in spatial analysis, were used. Isotropy, uniformity of variance in all directions, was also assumed. The exponential covariance function is parameterized as:

$$M(z_i, z_j) = \sigma^2 \exp\left(-\frac{\|z_i - z_j\|}{\alpha}\right) \tag{2}$$

The Matérn covariance function is parameterized as:

$$M(z_i, z_j) = \frac{\sigma^2 2^{1-\nu}}{\Gamma(\nu)} \left(\frac{\|z_i - z_j\|}{\alpha}\right)^\nu K_\nu\left(\frac{\|z_i - z_j\|}{\alpha}\right) \tag{3}$$

Covariance parameters are variance, σ^2, range, α, smoothness, ν and nugget, τ^2, for two GNSS co-ordinates z_i and z_j. The nugget value $\sigma^2\tau^2$ is added to the diagonal of the covariance matrix. Γ is a gamma function and K_ν is the modified Bessel function of the second

Table 1 Studies that used rasterized yield maps, based on yield monitor data, for various row crops toward analysis of spatial variability of crop yield

Citation	Methodologies	Usage	Other data layers	Data
Basso et al. (2007)	Kriging with exponential isotropic co-variance function	Delineating management zones	None	4 site-years of corn grain, soybean and wheat (8 ha) from Italy
Blackmore (2000)	Simple averaging	Delineating management zones	None	6 site-years of wheat (6.7 ha) from the United Kingdom
Brock et al. (2005)	Inverse distance weighting	Delineating management zones	None	24 site-years of corn and soybean from (45 ha) from the United States (US)
Buttafuoco et al. (2017)	Ordinary kriging	Delineating management zones	Soil characteristics	3 site-years of durum wheat (12 ha) from Italy
Diker et al. (2004)	Inverse distance weighting (12 nearest points)	Delineating management zones	None	6 site-years of commercial corn grain (123.4 ha) from US
Kharel et al. (2019a)	Inverse distance weighting	Delineating management zones	None	847 site-years of corn grain and silage (9084 ha) from US
Hornung et al. (2006)	Median polish kriging	Delineating management zones	Soil aerial imagery and field topology	3 site-years of corn (183 ha) from US
Khosla et al. (2008)	Ordinary kriging	Delineating management zones	Soil topology	15 site-years of corn grain from US
Cox and Gerrard (2007)	Nearest neighbor	Understanding interaction between yield and soil	None	12 site-years of soybean (39.4 ha) from US
Anderson-Cook et al. (2002)	Nearest neighbor	Understanding interaction between yield and soil	Electromagnetic conductivity (EC) maps	2 site-year of corn grain, barley, wheat and soybean (24 ha) from US
Kitchen et al. (1999)	Ordinary kriging	Understanding interactions between yield, soil and landscape	Electromagnetic conductivity (EC) maps	5 site-years of corn grain, 7 site-years of soybean and 1 site-year of grain sorghum (90 ha) from US
Maestrini and Basso (2018a)	Kriging with spherical isotropic co-variance function	Understanding yield variation	Red band spectral reflectance, NDVI and surface temperature	1625 site-years of corn grain, wheat, soybean and cotton
Yang et al. (2001)	Inverse distance weighting	Understanding yield and plant growth variation	Airborne digital imagery	1 site-year of sorghum (17 ha) from US
Maestrini and Basso (2018b)	Not mentioned	Understanding interactions between yield and climate, soil, topography and management	Publicly available data on topography, rain and soil information	1625 site-years of corn grain, soybean, wheat and cotton from US

kind. Unlike kriging, which incurs expensive computation time, NN and IDW require computation of distances between sample points only, resulting in reduced computational complexity compared to kriging. However, both NN and IDW fail to account for complex spatial correlation within a field. Nearest neighbor becomes especially inadequate when there is high noise in the data (Wettschereck 1994). While kriging is able to account for a complex correlation structure in the data, it incurs expensive computation time and is therefore less effective when only a weak spatial dependence is present in the data.

Numerous articles have been published comparing the performance of NN, IDW and kriging on a variety of data types. For example, Philips et al. (1997) and Grim and Lynch (1991) both used atmospheric data to quantify ozone exposure on forests and estimate wet deposition in the atmosphere, respectively. Berman et al. (2015) also evaluated the performances of kriging and inverse distance weighting on interpolating ozone concentrations. Various spatial interpolation methods also were compared using soil information data, such as clay content, soil organic carbon or pH (Bhunia et al. 2018; Bregt 1992; Brus et al. 1996; Declercq 1996; Gallichand and Marcotte 1993; Laslett et al. 1987; Laslett and McBratney 1990; Van Meirvenne et al. 1994). Studies by Heine (1986), Laslett (1994), Rouhani (1986) and Weber and Englund (1994) used (water) elevation data, while Kitanidis and Shen (1996) used chemical data such as, trichloroethylene concentration, to extrapolate spatially limited contaminant concentration information at a hazardous waste site into maps. Out of aforementioned sixteen studies, nine studies (Berman et al. 2015; Bhunia et al. 2018; Grim and Lynch 1991; Heine 1986; Laslett 1994; Laslett and McBratney 1990; Laslett et al. 1987; Philips et al. 1997; Rouhani 1986) compared the performance of kriging and IDW and concluded that kriging is the better methodology. Declercq (1996) showed IDW to be superior to kriging and five studies (Bregt 1992; Brus et al. 1996; Gallichand and Marcotte 1993; Weber and Englund 1994; Van Meirvenne et al. 1994) showed little difference in performance between kriging and IDW.

While there are numerous studies on comparison of spatial estimation methods in other research disciplines, there have been only a few studies comparing different spatial estimation methods for creating a regularized crop yield map based on yield monitor data. No method is uniformly superior on all data types and it therefore is important to systematically compare methods on grain and silage data. Dobermann and Ping (2004) used corn grain and soybean (*Glycine max*. (L.) Merr.) yield data, along with vegetation indices, to analyze the effectiveness of various kriging methods. Evaluated methods included ordinary kriging, co-kriging and kriging with external drift. The study concluded that ordinary kriging led to the lowest error (Dobermann and Ping 2004). Bazzi et al. (2015) derived profit maps from yield and economic data, such as sales price and production cost, for corn grain and soybean. Their analysis suggested that the impact of spatial estimation method (kriging versus IDW and IDW squared) on profit maps was less than US\$30 ha^{-1}, considered insignificant in their study (Bazzi et al. 2015). Souza et al. (2016) concluded that corn grain and soybean yield data lacked spatial structure and, hence, kriging did not outperform IDW. It is important to note, however, that all three studies had limited datasets. All three studies focused on corn grain and/or soybean data. Dobermann and Ping (2004) used data from just two site-years. Bazzi et al. (2015) and Souza et al. (2016) used data from four site-years. None of the studies used kriging with advanced covariance functions, such as exponential and Matérn covariance functions, which is expected to produce an improved raster map. In addition, studies on forages such as corn silage are lacking.

The objective was to evaluate seven widely used spatial estimation methods in creating a rasterized corn silage or grain yield map to determine the most accurate spatial estimation method that captures intra-field spatial variability of yield for both corn silage and

corn grain in the state of New York. Evaluation was done using corn silage yield monitor data from 7484 ha (245 fields) and corn grain yield data from 6971 ha (253 fields). The seven methods are: NN, IDW using 10, 20, 30 and all data points (IDW 10, 20, 30 and All, respectively) and kriging with exponential (Exponential) and Matérn covariance function (Matérn). The hypothesis is that of the seven methods evaluated, kriging with Matérn covariance function results in the smallest percent error regardless of field size, year when data are obtained or source of the data (farm) for both silage and grain data.

Materials and methods

Yield monitor datasets

Yield monitor data were collected from 1318 site-years from four farms, two of which were dairy farms (hereafter referred to as Silage A and B) and two were cash grain operations (hereafter referred to as Grain A and B). Silage A and B supplied ten and nine years of data, respectively, for a total area of 7484 ha. Grain A and B supplied seven and eight years of data, respectively, for a total of 6971 ha. Data reflected the large variability in both yield and field size within farms in New York (Table 2; Fig. 1).

Postharvest yield data cleaning

Yield monitor data need to be cleaned before analysis because of the presence of systematic and random errors in the data (Dobermann and Ping 2004; Vega et al. 2019). The raw yield monitor data were read in SMS Advanced software (Ag Leader Technology, Ames, IA, USA), exported in AgLeader format, and imported into and cleaned with Yield Editor (Sudduth et al. 2012; Sudduth and Drummond 2007) using a standardized post-harvest data cleaning protocol (Kharel et al. 2018). This data cleaning protocol addresses issues related to pass overlap (driving over areas already harvested) and yield extremes and applies sensor delays (flow delay and moisture delay) to match the position of sensors with the harvester location based on the flow or moisture pattern within the field and start- and end-pass delays to eliminate inaccurate readings when the harvester is speeding up or slowing down. With the data cleaning protocol, 19, 24, 21 and 21% of data were removed for Silage A, B, Grain A and B, respectively. These values are consistent with Blackmore (1999) who removed 32%, Vega et al. (2019) who removed 30% and Thylén et al. (2000) who removed 10–50% of the erroneous yield monitor data.

Implementation of spatial estimation methods

The seven spatial estimation methods explored in this paper include NN, IDW with 10 (IDW 10), 20 (IDW 20), 30 (IDW 30) and all data points (IDW All), kriging with an exponential isotropic covariance function (Exponential) and kriging with the Matérn isotropic covariance function (Matérn), reflecting common methods used in other studies. The data were split into a training (80% of the data) and cross-validation datasets (remaining 20% of the data). Data analyses were performed with R (R Core Team 2019). Gstat package (Pebesma 2004) was used to implement NN and IDW. The GpGp package (Guinness and Katzfuss 2019) was used to implement kriging in order to reduce processing time, given the large number of data points. One of the difficulties in implementing kriging is the

computation time. As Katzfuss and Guinness (2019) suggest, kriging becomes infeasible as the size of the dataset becomes larger. This is because kriging requires computation of multivariate normal distributions which incurs quadratic memory and cubic time complexity in the number of observations. In the dataset, fields averaged 6358 data points, with a maximum of 59 971 data points per field. Implementation of kriging through the "gstat" package, therefore, was not feasible. Parameters for kriging were estimated through maximum likelihood estimation. Unlike the gstat package, the GpGp package uses a generalization of the Vecchia (1988) approach as a framework for Gaussian Process (GP) approximation, which enables fast evaluation of likelihood function resulting in shorter overall computation time.

Spatial estimation methods evaluation

Cross validation was performed to evaluate the performance of each spatial estimation method. For each field, 80% of the data were randomly selected for training. The training dataset was used to generate rasterized yield maps at 2×2 m spatial resolution using the various spatial estimation methods. Predictions were then compared against the validation data. Two evaluation schemes were explored: point-based and area-based. In the point-based approach, the actual yield value from the validation set was compared to the yield from the predicted rasterized yield map at the given GNSS co-ordinate. While point-based evaluation is a natural approach for validating point estimates, the approach fails to acknowledge that yield monitor data represent an average yield density over an area, instead of a point estimate at a given co-ordinate. Though the yield monitor system provides a yield estimate at a certain GNSS co-ordinate, the estimate does not represent a yield value at that specific location, but rather represent the average yield density over the distance traveled from the previous GNSS co-ordinate times the width of the harvest equipment. To correctly ascribe a yield estimate to an area, polygons were generated based on the equipment width, (swath) and distance traveled, as provided by the yield monitor. In the area-based evaluation, the actual yield value from the validation set was then compared against the average yield estimates of all 2×2 m pixels inside a given polygon. By accounting for the fact that a point estimate from the yield monitor represents an average yield density over a certain area, the goal was to represent yield monitor data more accurately. However, this approach was computationally expensive and more time consuming than the point-based approach. Both approaches were evaluated to determine if point-based evaluation is an appropriate approximation of area-based evaluation. Normalized root mean squared error (NRMSE) was used to evaluate the performance of each model per field. Assuming that there are m set of co-ordinates, denoted as $x_1, x_2, \ldots, x_m$, in the validation dataset of a particular field:

$$NRMSE = \frac{\sqrt{\frac{1}{m} \sum_{j=1}^{m} \left(Y(x_j) - \overline{Y}(x_j) \right)^2}}{\frac{1}{m} \sum_{j=1}^{m} Y(x_j)} \times 100 \qquad (4)$$

where $Y(x_j)$ represents the actual yield level at co-ordinate x_j and $\overline{Y}(x_j)$ represents the predicted yield level at co-ordinate x_j based on one of the methods. Because residuals, $Y(x_j) - \overline{Y}(x_j)$ for $i \in \{1, 2, \ldots, m\}$, are usually proportional to the yield level of that field, RMSE from a high yielding field will generally be larger than that of a lower yielding field, thus putting more weight on errors from high yielding fields. By normalizing RMSE with

Table 2 Summary of farm information illustrating years of record, number of fields, yield statistics, field size statistics, equipment information, location and soil type

	Unit	Dairyfarm A(Silage A)	Dairyfarm B(Silage B)	Grain operation A (Grain A)	Grain operation B (Grain B)
Years of record	Years	10	9	7	8
Number of fields		155	90	163	90
Field	ha				
Average field size		13.6	9.9	10.3	9.2
Smallest field		1.5	0.9	0.3	1.1
Largest field		109.5	60.7	53.5	30.7
Total area analyzed		5192.2	2291.7	3565.0	3406.2
Yield	Mg ha^{-1}				
Average yield[a]		49.5	46.4	10.3	11.7
Lowest yielding field		26.1	4.7	2.4	6.3
Highest yielding field		81.9	72.0	15.3	15.4
Average spatial stdev		8.4	8.0	2.6	2.2
Equipment					
Yield monitor		John Deere Greenstar 3	John Deere Greenstar 3	John Deere Greenstar 3	John Deere Greenstar 3
Recording interval	Second	1	1	1	1
Harvester width[b]	Rows	10, 12	10	8, 12	8, 12
Location		Central New York	Western New York	Central New York	Central New York
Soil type					
Most common		Honeoye (Fine-loamy, mixed, semiactive, mesic Glossic Hapludalfs)	Erie (Fine-loamy, mixed, active, mesic Aeric Fragiaquepts)	Schoharie (Fine, illitic, mesic Oxyaquic Hapludalfs)	Ontario (Fine-loamy, mixed, active, mesic Glossic Hapludalfs)
Second most common		Lima (Fine-loamy, mixed, semiactive, mesic Oxyaquic Hapludalfs)	Langford (Fine-loamy, mixed, active, mesic Typic Fragiudepts)	Dunkirk (Fine-silty, mixed, active, mesic Glossic Hapludalfs)	Hilton (Fine-loamy, mixed, active, mesic Oxyaquic Hapludalfs)

[a] Area weighted average yield

[b] Rows were 0.76 m apart
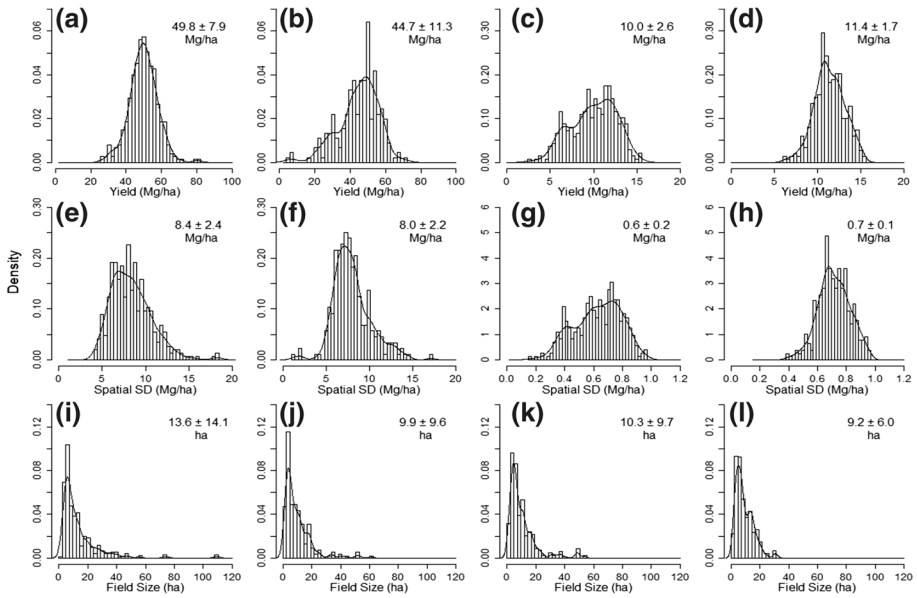
Fig. 1 Average yield per field (**a–d**), spatial standard deviation of yield (**e–h**) and field size (**i–l**) density distributions for corn silage (**a**, **b**, **e**, **f**, **i**, **j**) and corn grain (**c**, **d**, **g**, **h**, **k**, **l**) post data cleaning protocol. Results are presented for two dairy farms with silage data (Silage A and B) and two cash grain operations with corn grain data (Grain A and B), respectively, from the left to right

the average yield of the field, NRMSE provides a dimensionless measurement of error per field.

Empirical average analysis

Area-based evaluation resulted, on average, in a higher NRMSE than point-based evaluation. While the assumption that each observation of yield monitor data represents yield over an area rather than at a specific location is a sound data assumption, the seven spatial estimation methods explored in this paper all assume the data to be point estimates, rather than estimates over an area. This discrepancy contributed to over-estimation of error by the area-based evaluation. Thus, the empirical average analysis was performed based on point-based evaluation results only. The empirical averages of NRMSE of each spatial methods by data type (Silage A, Silage B, Grain A and Grain B), field size (up to 140 ha) and year (2009–2018) were analyzed and compared.

The analysis suggested that the average NRMSE of Grain A data was much larger than that of other three farms. Average coefficient of variation (CV) was calculated for each farm to compare variation of yield level per farm. Suppose that there are n set of co-ordinates, $z_1, z_2, \ldots, z_n$ and their yield values in a single field. Coefficient of variation (CV) is defined as:

$$CV = \frac{\sqrt{\frac{1}{n} \sum_{i=1}^{n} \left(Y(z_i) - \hat{Y} \right)^2}}{\hat{Y}} \tag{5}$$

where $\hat{Y}$ is the average yield level of the field. Average CV was derived by taking the arithmetic mean of CV of all fields within the farm. The relative performance of spatial methods were mostly consistent across data type, field size and year in which data were collected, except for the nearest neighbor method. The nearest neighbor method was further analyzed to account for such volatility in its performance. Coefficient of variation of yield, log of field size and year were analyzed to test the relationship between yield variability within a field and NRMSE using linear regression.

Mixed model analysis

For reasons explained above, the mixed model analysis was based on point-based evaluation results only. After analyzing behaviors of empirical averages of NRMSE, a mixed model was fitted using the "lme4" package in R (Bates et al. 2015) to compare differences in NRMSE for each spatial estimation methods and to test if they are statistically significant. The following R command was used to fit the linear mixed model:

$$lmer(\text{NRMSE} \sim \text{Method} * \log(\text{Area}) + \text{Farm} + \text{Year} + (1|\text{Field})) \tag{6}$$

where lmer refers to a R command to fit a linear mixed effect model in R; Method refers to the seven spatial estimation methods (Fixed effect); Area is the size of the field (Fixed effect); Farm refers to Grain A, Grain B, Silage A, Silage B (Fixed effect); Year reflects the year in which the harvest was done (Fixed effect); and Field reflects the unique combination of farm, fieldname and year of harvest (Random effect). In this model, "Area" was log transformed to normalize the data, as they were distinctly right skewed (as evident in Fig. 1). In addition to additive effects from "spatial estimation methods", "farm", "year" and "log(area)", multiplicative effects between "spatial estimation methods" and "log(area)" were introduced, because the effect of "log(area)" on NRMSE varied significantly depending on "spatial estimation methods". Marginal means were estimated for each spatial estimation method using the "lsmeans" package in R (Lenth 2016). Marginal means were estimated by adding average fixed effects over 10 years, 4 farms and average field size of 11 ha to the intercept for each spatial estimation method. Tukey comparisons were then performed between spatial estimation methods to elucidate the statistical difference in model performance.

Results and discussion

Area- versus point-based evaluation

Across IDW- and kriging-based spatial estimation methods and all fields and farms, area-based evaluation consistently led to a slightly higher average NRMSE, averaging 8.6 across these methods versus 7.9 for the point-based evaluation (Table 3). The most likely reason for larger NRMSE in area-based evaluation in these estimation models is that none of these spatial estimation methods account for the fact that each observation from a yield monitor system is an estimate for a certain area (product of harvester width and distance traveled per second) and not an actual point estimate with specific GNSS units.

Under both evaluation methods, Matérn consistently showed the lowest average NRMSE among all seven spatial methods, with 7.1 error under area-based evaluation and 6.6 error under point-based evaluation. Exponential resulted in the second lowest average NRMSE,

followed by IDW 10, IDW 20, IDW 30 and IDW All. The estimation accuracy of IDW deteriorated with an increasing number of data points, which is plausibly due to increased smoothing as data points farther from the estimation location are captured. Performance of NN, on the other hand, varied by evaluation method. Under area-based evaluation, NN was the third best performing method behind Matérn and Exponential. Under point-based evaluation, however, NN was the fifth best method for Silage A and Grain A data, fourth best for Grain B data and sixth best on Silage B data. Given that both area- and point-based evaluations yielded the same results, with a slightly lower NRMSE for point-based evaluation for most comparisons, additional analyses on the impact of field size, year and farm specificity on model performance were performed using the point-based evaluation method for both corn silage and corn grain data.

Performance of spatial estimation methods by farm, field, year and field size

The empirical average NRMSE per farm ranged from 5 to 9 for Silage A, B and Grain B, and from 9 to 14 for Grain A (Table 3). This could be explained by the higher variation of yield on average for Grain A data. Coefficient of variation of yield, a measure of variation in yield per field, was calculated for each farm. Grain A had higher average CV of 27% whereas Silage A, Silage B and Grain B had 17, 19 and 20% respectively, suggesting higher level of yield variation for Grain A data, which could result in higher NRMSE across all seven methods. However, despite an overall higher NRMSE for Grain A, the evaluation of the seven spatial estimation methods on this farm still resulted in the same ranking of methods: Matérn was the best performing method with the lowest average NRMSE, followed by Exponential, IDW 10, IDW 20, IDW 30 and IDW All. The NN results were inconsistent; it was the 2nd lowest method behind IDW All for Grain B, the 3rd lowest method behind IDW All and IDW 30 for Silage A and Grain A, and 4th lowest behind IDW All, IDW 30 and IDW 20 for Silage B.

At the individual field level, the NRMSE from Matérn was also consistently lower than that of other spatial estimation methods (Fig. 2) as most observations, which represent NRMSE from Matérn on the y-axis and NRMSE from other models on the x-axis, on the plot are on the right hand side of the one-to-one line. Thus, not only across farms but also across individual fields, Matérn was the best performing method.

The average NRMSE ranged between 6.1 and 8.9, year-to-year. Despite the difference in NRMSE year-to-year, the relative performance of the spatial estimation methods, except NN, were consistent across years; Matérn always resulted in the lowest NRMSE, followed by Exponential, IDW 10, IDW 20, IDW 30 and IDW All (Fig. 3). The results of the NN method showed inconsistency in ranking from year-to-year; while in most years (2011, 2014, 2016, 2017 and 2018), the NN method was one of the lowest performing methods, next to IDW All. In 2009, it was the third best method behind Matérn and Exponential. However, for every year of data and for both crop types, Matérn outperformed all other methods.

In general, all seven spatial estimation methods performed better as the size of the field increased (Fig. 4). The degree to which NRMSE decreases as the size of the field increases differed among methods; IDW had the least steep slope of -0.64, while NN had the steepest slope of -0.99. Despite this difference in slope among spatial estimation methods, Matérn resulted in the lowest average NRMSE across fields, followed by Exponential, IDW 10, IDW 20, IDW 30 and IDW All.

Table 3 Comparison of average Normalized Root Mean Squared Errors (NRMSE) by farm (Silage A, Silage B, Grain A and Grain B) and evaluation methods (area-based and point-based) for seven spatial estimation methods

| Spatial estimation methods	Silage A		Silage B		Grain A		Grain B	
	Area	Point	Area	Point	Area	Point	Area	Point
Nearest neighbor (NN)	6.94	6.89	7.55	7.76	9.73	10.74	5.84	6.72
Inverse distance weighting (IDW)								
10 nearest points (IDW 10)	7.34	6.37	7.59	6.97	10.40	9.94	6.65	6.41
20 nearest points (IDW 20)	7.94	6.78	8.19	7.22	11.18	10.46	7.25	6.86
30 nearest points (IDW 30)	8.26	7.02	8.52	7.39	11.61	10.78	7.57	7.12
All data points (IDW All)	10.60	9.13	11.20	9.26	15.20	14.05	10.06	9.47
Kriging								
Exponential isotropic (Exponential)	6.49	5.63	7.22	6.59	9.70	9.29	5.82	5.49
Matérn isotropic (Matérn)	6.10	5.42	7.14	6.54	9.53	9.19	5.31	5.14

Estimated marginal means were generated (with point-based evaluation only) for comparisons between spatial estimation methods

The analysis suggests that the performance of the NN varies by field. Wettschereck (1994) analyzed behavior of the k-nearest neighbor algorithm (1, 2… k) on various data containing noisy instances and discovered that the performance of the NN algorithm depended on number, noisiness and sparseness of the instances. He showed that NN performed poorly especially on larger dataset (> 100 data points), while performing better on smaller (< 100 data points) or sparsely distributed dataset. This is in line with the observation for the NN algorithm in the analysis. Sparseness, number and noisiness of instances varied greatly by field, causing the performance of the NN method to also vary. While the performance of NN varied by field, for point-based evaluation, Matérn resulted in the lowest NRMSE for all but one of the 1318 fields (Fig. 2).

The strong effects of field size and year on the NRMSE were attributed to the yield variation within a field. The regression of CV in yield of each field and log of field size suggested that as the field size increased the CV decreased (Table 4). The regression of CV of yield and year indicated that the data from 2018 had the lowest variation in yield (Table 4). The correlation between CV and NRMSE showed a linear relationship between NRMSE and CV across fields (Fig. 5), supporting the hypothesis that variation in yield affects the accuracy of all methods.

Mixed model results

Consistent with the observations of empirical averages, T-statistics and p-values from the mixed model indicated statistical significance of all the beta estimates in the model (Table 5). Kriging with the Matérn isotropic covariance function (Matérn) resulted in the lowest estimated marginal means of 6.6 error, followed by Exponential with 6.7 error, IDW 10 with 7.3 error, IDW 20 with 7.7 error, NN with 7.9 error, IDW 30 with 8.0 error and IDW All with 10.4 error (Table 6). In all pairwise comparisons between Matérn and six other spatial methods, the difference in NRMSE was statistically significant ($p < 0.0001$) (Table 7).
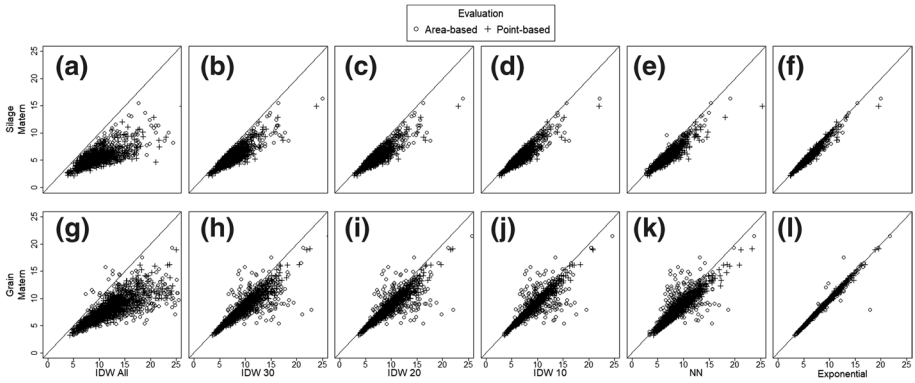
Fig. 2 Comparison of normalized root mean squared error (NRMSE) per field. Each point on a plot represents NRMSE of a field for corn silage (**a–f**) and corn grain (**g–l**). Each dot represents NRMSE from area-based evaluation and a cross represents NRMSE from point-based evaluation. Spatial estimation methods included nearest neighbor (NN), inverse distance weighting (IDW) with varying number of nearest points (10, 20, 30, all) and kriging with exponential (Exponential) or Matérn (Matérn) covariance functions

On average, NRMSE from Matérn was 17% lower than NRMSEs of the other six spatial estimation methods. The difference was the largest with 37% decrease when compared against IDW All and the smallest when compared against Exponential with just 2% decrease. These results suggest kriging to be the most consistent spatial estimation method in mapping yield monitor data for corn grain and silage across a large range of field sizes and yield levels. Contrary to the finding by Souza et al. (2016) that yield monitor data lack spatial structure, the result suggests that spatial information can be used to better estimate yield at the field- and within-field levels for both corn grain and silage. The results
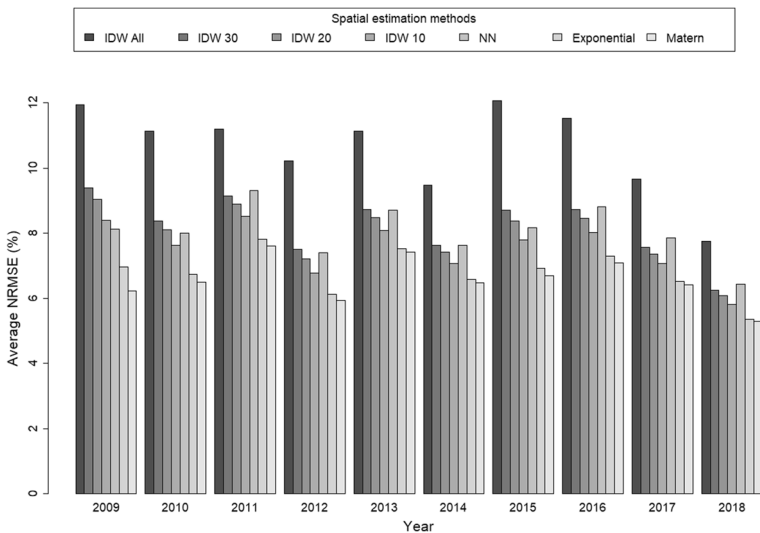
Fig. 3 Comparison of average normalized root mean squared error from year 2009–2018 for each spatial estimation method, including nearest neighbor (NN), inverse distance weighting (IDW) with varying number of nearest points and kriging with exponential (Exponential) or Matérn (Matérn) covariance functions

also contradict Bazzi et al. (2015), who stated that the spatial estimation method was of peripheral importance in generating a yield map. The contradictory results may stem from varying data cleaning protocol, such effects were not tested. The analysis shows that the difference between Matérn, the best performing method, and IDW All, the lowest performing model, averaged 46% per field, suggesting that spatial estimation method is a significant factor when generating a yield map. Both Souza et al. (2016) and Bazzi et al. (2015) included only a limited number of fields and focused on grain crops (soybean and corn). The apparent inconsistency in conclusions between this study and the work by Souza et al. (2016) and Bazzi et al. (2015) may be due to differences in location and the size and source of the data, including crop type.

A rasterized yield map based on yield monitor data often is used, along with other data, such as vegetation indices or electrical conductivity maps, to delineate management zones (Basso et al. 2007; Blackmore 2000; Brock et al. 2005; Diker et al. 2004; Hornung et al. 2006; Kharel et al. 2018; Khosla et al. 2008) or to understand the interaction between yield and other features such as soil, landscape and topography (Anderson-Cook et al. 2002; Cox and Gerrard 2007; Kitchen et al. 1999; Maestrini and Basso 2018b; Yang et al. 2001). Out of the 12 studies listed above, only five studies (Basso et al. 2007; Hornung et al. 2006; Khosla et al. 2008; Kitchen et al. 1999; Maestrini and Basso 2018b) used a form of kriging to generate a rasterized yield map. The analysis suggests that greater attention is required to yield mapping by both researchers and practitioners who aim to use yield data to develop management zones and/or prescription maps, given that the choice of estimation method affects the rasterized yield maps generated from the yield monitor data. Findings in this
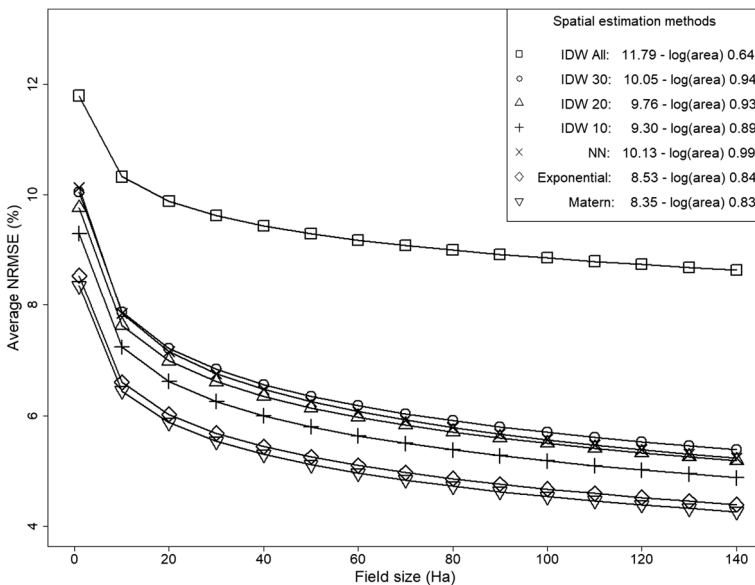

Fig. 4 Comparison of average normalized root mean squared error (NRMSE) by corn field size, ranging up to 140 ha for each spatial estimation method, including nearest neighbor (NN), inverse distance weighting (IDW) with varying number of nearest points and kriging with exponential (Exponential) or Matérn (Matérn) covariance functions. A regular linear regression model with NRMSE as the dependent and log of area in hectare as the independent variable was fitted for each spatial estimation method to analyze the performances conditioned on field sizes

Table 4 Summary of linear model based on two independent variables

Term	Estimate	Standard Error	T-statistics	P-value
(Intercept)	0.261	0.011	22.969	<0.001
log(field size)	−0.023	0.003	−8.298	<0.001
Year2009	0	–	–	–
Year2010	−0.039	0.011	−3.482	0.001
Year2011	0.028	0.011	2.442	0.015
Year2012	−0.001	0.012	−0.116	0.908
Year2013	0.010	0.012	0.808	0.419
Year2014	0.027	0.012	2.300	0.022
Year2015	−0.017	0.012	−1.509	0.132
Year2016	−0.006	0.032	−0.204	0.838
Year2017	0.016	0.012	1.264	0.207
Year2018	−0.056	0.012	−4.609	<0.001

Year implies the year when the data were collected and log(field size) implies a log-transformed field size. The dependent variable was the coefficient of variation of yield on each field (CV), which was calculated by averaging the standard deviation of yield by the average yield of the field. The summary output shows beta estimates, standard errors, T-statistics and P-Values

Fig. 5 Comparison of normalized root mean squared error (NRMSE) across seven spatial estimation methods and average coefficient of variation in yield for 1318 corn fields
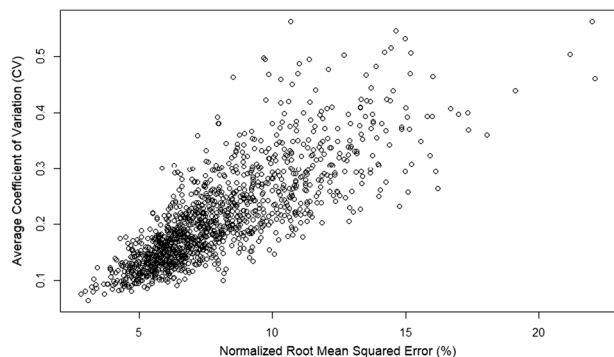
paper span a large number of fields, variety in field sizes and yield levels, as well as corn harvested for grain and corn grown for silage and suggest the need for kriging with Matérn isotropic covariance function to account for the spatial structure of yield within fields.

Conclusions

Out of the seven spatial estimation methods tested, kriging with Matérn isotropic covariance function resulted in the lowest NRMSE across four farms, ten years of silage yield data, nine years of grain yield data and across a wide range of field sizes (1–140 ha), reflecting the diversity of fields in corn production in New York. On average, Exponential was the second-best method, followed by IDW 10, IDW 20, NN, IDW 30 and IDW All. These results support the original hypothesis. Kriging with Matérn covariance function is

Table 5 Linear mixed effect model summary for 7–10 years of data per farm (7484 ha [245 fields] of silage and 6971 ha [253 fields] of grain) from four farms (Grain A and B, Silage A and B), where Method refers to seven spatial estimation methods (Fixed effect); log(Area) implies a log-transformed field size (Fixed effect); Farm refers to Grain A, B, Silage A, B (Fixed effect); Year reflects year of harvest (Fixed effect); and Field reflects the unique combination of farm, fieldname and harvest year (Random effect)

	Estimate	Standard Error	Degrees of Freedom	T value	P value
[Intercept]	13.05	0.79	1333	16.55	<0.001
Models [IDW All]	0.00	–	–	–	–
Models [IDW 30]	−1.46	0.13	7896	−11.69	<0.001
Models [IDW 20]	−1.77	0.13	7896	−14.09	<0.001
Models [IDW 10]	−2.26	0.13	7896	−18.01	<0.001
Models [NN]	−1.34	0.13	7896	−10.69	<0.001
Models [Exponential]	−3.07	0.13	7896	−24.53	<0.001
Models [Matérn]	−3.26	0.13	7896	−26.05	<0.001
log(Area)	−0.57	0.08	1702	−7.55	<0.001
Farm [Silage A]	0.00	–	–	–	–
Farm [Silage B]	−0.35	0.17	1304	−2.05	0.040
Farm [Grain A]	3.63	0.16	1304	22.46	<0.001
Farm [Grain B]	0.41	0.15	1304	2.75	0.006
Year [2009]	0.00	–	–	–	–
Year [2010]	−1.94	0.80	1304	−2.43	0.015
Year [2011]	−0.86	0.78	1304	−1.11	0.266
Year [2012]	−1.67	0.78	1304	−2.14	0.032
Year [2013]	−1.68	0.78	1304	−2.16	0.031
Year [2014]	−2.86	0.77	1304	−3.70	<0.001
Year [2015]	−1.42	0.77	1304	−1.84	0.066
Year [2016]	−1.66	0.77	1304	−2.16	0.031
Year [2017]	−1.81	0.77	1304	−2.35	0.019
Year [2018]	−2.69	0.77	1304	−3.48	0.001
Models [IDW All]: log(Area)	0.00	–	–	–	–
Models [IDW 30]: log(Area)	−0.31	0.04	7896	−7.55	<0.001
Models [IDW 20]: log(Area)	−0.29	0.04	7896	−7.09	<0.001
Models [IDW 10]: log(Area)	−0.26	0.04	7896	−6.33	<0.001
Models [NN]: log(Area)	−0.35	0.04	7896	−8.70	<0.001
Models [Exponential]: log(Area)	−0.20	0.04	7896	−4.94	<0.001
Models [Matérn]: log(Area)	−0.19	0.04	7896	−4.69	<0.001
Random Effects					
Residual (σ^2)	0.69				
Intercept [Field] (τ_{Field})	3.84				
Number of observations for Field	1318				
Total number of observations	9226				

The summary output shows beta coefficients, standard errors, degrees of freedom, t and p values for the fixed effects, as well as the residual and group variances of the random effects

Table 6 The least square mean estimates, their respective standard errors and 95% confidence intervals of normalized root mean squared error (NRMSE) for seven spatial estimation methods

Spatial estimation methods	Estimates	Standard Error	95% confidence interval
Nearest neighbor (NN)	7.94	0.10	7.75–8.13
Inverse distance weighting (IDW)			
10 nearest points (IDW 10)	7.34	0.10	7.15–7.53
20 nearest points (IDW 20)	7.73	0.10	7.54–7.92
30 nearest points (IDW 30)	7.97	0.10	7.77–8.16
All data points (IDW All)	10.44	0.10	10.25–10.64
Kriging			
Exponential isotropic (Exponential)	6.71	0.10	6.52–6.90
Matérn isotropic (Matérn)	6.55	0.10	6.36–6.74

The response for the linear mixed model was NRMSE; four farms (Grain A, B, Silage A, B), the seven spatial estimation methods, harvest year (2009~2018) and the logged transformed size of the field in hectare were treated as additive fixed effects

Table 7 Tukey comparison of least square estimates of normalized root mean squared error (NRMSE) between kriging with Matérn isotropic covariance function (Matérn) and six other methods, including inverse distance weighting (IDW) with varying number of points, nearest neighbor (NN) and kriging with exponential isotropic covariance function (Exponential)

Contrast	Estimate	Standard Error	Z ratio	P-value
IDW All—Matérn	3.892	0.035	111.854	< 0.0001
IDW30—Matérn	1.415	0.035	40.679	< 0.0001
IDW20—Matérn	1.176	0.035	33.810	< 0.0001
IDW10—Matérn	0.787	0.035	22.629	< 0.0001
NN—Matérn	1.387	0.035	39.860	< 0.0001
Exponential—Matérn	0.156	0.035	4.497	< 0.0001

highly recommended to derive single year corn yield raster maps for corn grain and corn silage yield monitor data and development of multi-year yield stability maps that include not only spatial, but also temporal variation in yield.

Compliance with ethical standards

Conflict of interest The authors declare that they have no conflict of interest.

References

Anderson-Cook, C. M., Alley, M. M., Roygard, J. K. F., Khosla, R., Noble, R. B., & Doolittle, J. A. (2002). Differentiating soil types using electromagnetic conductivity and crop yield maps. *Soil Science Society of America Journal, 66,* 1562–1570. https://doi.org/10.2136/sssaj2002.1562.

Arslan, S., & Colvin, T. (2002). An evaluation of the response of yield monitors and combines to varying yields. *Precision Agriculture, 3,* 107–122. https://doi.org/10.1023/A:1013887801918.

Basso, B., Bertocco, M., Sartori, L., & Martin, E. C. (2007). Analyzing the effects of climate variability on spatial pattern of yield in a maize–wheat–soybean rotation. *European Journal of Agronomy, 26*(2), 82–91. https://doi.org/10.1016/j.eja.2006.08.008.

Bates, D., Maechler, M., Bolker, B., & Walker, S. (2015). Fitting linear mixed-effects models using lme4. *Journal of Statistical Software, 67*(1), 1–48. https://doi.org/10.18637/jss.v067.i01.

Bazzi, C. L., Souza, E. G., Khosla, R., Uribe-Opazo, M. A., & Schenatto, K. (2015). Profit maps for precision agriculture. *Ciencia e investigación agraria, 42*(3), 305–330. https://doi.org/10.4067/S0718-16202015000300007.

Berman, J. D., Breysse, P. N., White, R. H., Darryn, W. W., & Curriero, F. C. (2015). Evaluating methods for spatial mapping: Applications for estimating ozone concentrations across the contiguous United States. *Environmental Technology & Innovation, 3,* 1–10. https://doi.org/10.1016/j.eti.2014.10.003.

Bhunia, G. S., Shit, P. K., & Maiti, R. (2018). Comparison of GIS-based interpolation methods for spatial distribution of soil organic carbon (SOC). *Journal of the Saudi Society of Agricultural Sciences, 17*(2), 114–126. https://doi.org/10.1016/j.jssas.2016.02.001.

Blackmore, S. (1999). Remedial correction of yield map data. *Precision Agriculture, 1,* 53–66. https://doi.org/10.1023/A:1009969601387.

Blackmore, S. (2000). The interpretation of trends from multiple yield maps. *Computers and Electronics in Agriculture, 26*(1), 37–51. https://doi.org/10.1016/S0168-1699(99)00075-7.

Bregt, A. K. (1992). *Processing of soil survey data*. Ph.D. thesis, Department of Environmental Sciences, Agricultural University of Wageningen, The Netherlands.

Brock, A., Brouder, S. M., Blumhoff, G., & Hofmann, B. S. (2005). Defining yield-based management zones for corn-soybean rotations. *Agronomy Journal, 97*(4), 1115–1128. https://doi.org/10.2134/agronj2004.0220.

Brus, D. J., DeGruijter, J. J., Marsman, B. A., Visschers, R., Bregt, A. K., & Breeuwsma, A. (1996). The performance of spatial interpolation methods and choropleth maps to estimate properties at points: A soil survey case study. *Environmetrics, 7,* 1–16. https://doi.org/10.1002/(sici)1099-095x(199601)7:1%3c1::aid-env157%3e3.0.co;2-y.

Buttafuoco, G., Castrignanò, A., Cucci, G., Lacolla, G., & Lucà, F. (2017). Geostatistical modelling of within-field soil and yield variability for management zones delineation: A case study in a durum wheat field. *Precision Agriculture, 18,* 37–58. https://doi.org/10.1007/s11119-016-9462-9.

Cox, M., & Gerard, P. (2007). Soil management zone determination by yield stability analysis and classification. *Agronomy Journal, 99,* 1357–1365. https://doi.org/10.2134/agronj2007.0041.

Declercq, F. A. N. (1996). Interpolation methods for scattered sample data: Accuracy, spatial patterns, processing time. *Cartography and Geographic Information Systems, 23*(3), 128–144. https://doi.org/10.1559/152304096782438882.

Diker, K., Heermann, D., & Brodahl, M. (2004). Frequency analysis of yield for delineating yield response zones. *Precision Agriculture, 5,* 435–444. https://doi.org/10.1007/s11119-004-5318-9.

Dobermann, A., & Ping, J. (2004). Geostatistical integration of yield monitor data and remote sensing improves yield maps. *Agronomy Journal, 96,* 285–297. https://doi.org/10.2134/agronj2004.0285.

Gallichand, J., & Marcotte, D. (1993). Mapping clay content for subsurface drainage in the Nile Delta. *Geoderma, 58,* 165–179. https://doi.org/10.1016/0016-7061(93)90040-r.

Grim, J. W., & Lynch, J. A. (1991). Statistical analysis of errors in estimating wet deposition using five surface estimation algorithms. *Atmospheric Environment Part A, 26*(2), 317–327. https://doi.org/10.1016/0960-1686(91)90303-o.

Guinness, J., & Katzfuss, M. (2019) *GpGp: Fast Gaussian Process Computation Using Vecchia's Approximation.* R package version 0.2.1 Retrieved August 19, 2020, from https://CRAN.R-project.org/package=GpGp.

Heine, G. W. (1986). A controlled study of some two-dimensional interpolation methods. *COGS Computer Contributions, 2*(2), 60–72.

Hornung, A., Khosla, R., Reich, R., Inman, D., & Westfall, D. (2006). Comparison of site-specific management zones: Soil-color-based and yield-based. *Agronomy Journal, 98*(2), 405–417. https://doi.org/10.2134/agronj2005.0240.

Katzfuss, M., & Guinness, J. (2019). A general framework for Vecchia Approximations of Gaussian processes. Retrieved June 29, 2020, from non-peer reviewed preprint at https://arxiv.org/abs/1708.06302.

Kharel, T., Swink, S. N., Youngerman, C., Maresma, A., Czymmek, K. J., Ketterings, Q. M., et al. (2018). *Processing/cleaning corn silage and grain yield monitor data for standardized yield maps across farms, fields, and years*. Ithaca, NY, USA: Cornell University, Nutrient Management Spear Program, Department of Animal Science. Retrieved August 19, 2020, from http://nmsp.cals.cornell.edu/publications/extension/ProtocolYieldMonitorDataProcessing1_15_2020.pdf.

Kharel, T. P., Marema, A., Czymmek, K. J., Oware, E. K., & Ketterings, Q. M. (2019a). Combining spatial and temporal corn silage yield variability for management zone development. *Agronomy Journal, 111*(6), 2703–2711. https://doi.org/10.2134/agronj2019.02.0079.

Kharel, T. P., Swink, S. N., Maresma, A., Youngerman, C., Kharel, D., Czymmek, K. J., et al. (2019b). Yield monitor data cleaning is essential for accurate corn grain/silage yield determination. *Agronomy Journal, 111*(2), 509–516. https://doi.org/10.2134/agronj2018.05.0317.

Kitanidis, P. K., & Shen, K. F. (1996). Geostatistical interpolation of chemical data. *Advances in Water Resources, 19,* 369–378. https://doi.org/10.1016/0309-1708(96)00016-4.

Kitchen, N. R., Sudduth, K. A., & Drummond, S. T. (1999). Soil electrical conductivity as a crop productivity measure for claypan soils. *Journal of Production Agriculture, 12*(4), 607–617. https://doi.org/10.2134/jpa1999.0607.

Khosla, R., Inman, D. J., Westfall, D. G., Reich, R. M., Frasier, M., Mzuku, M., et al. (2008). A synthesis of multi-disciplinary research in precision agriculture: Site-specific management zones in the semi-arid western Great Plains of the USA. *Precision Agriculture, 9,* 85–100. https://doi.org/10.1007/s11119-008-9057-1.

Laslett, G. M., McBratnety, A. B., Pahl, P. J., & Hutchinson, M. F. (1987). Comparison of several spatial prediction methods for soil pH. *Journal of Soil Science, 38,* 325–341. https://doi.org/10.1111/j.1365-2389.1987.tb02148.x.

Laslett, G. M. (1994). Kriging and splines: An empirical comparison of their predictive performance in some applications. *Journal of the American Statistical Association, 89,* 391–409. https://doi.org/10.2307/2290840.

Laslett, G. M., & McBratney, A. B. (1990). Further comparisons of spatial methods for predicting soil pH. *Soil Society of America Journal, 54,* 1553–1558. https://doi.org/10.2136/sssaj1990.03615995005400060007x.

Lenth, R. V. (2016). Least-squares means: The R Package lsmeans. *Journal of Statistical Software, 69*(1), 1–33. https://doi.org/10.18637/jss.v069.i01.

Long, E., Ketterings, Q. M., Russell, D., Vermeylen, F., & DeGloria, S. D. (2016). Assessment of yield monitoring equipment for dry matter and yield of corn silage and alfalfa/grass. *Precision Agriculture, 7,* 546–563. https://doi.org/10.1007/s11119-016-9436-y.

Maestrini, B., & Basso, B. (2018a). Drivers of within-field spatial and temporal variability of crop yield across the US Midwest. *Scientific Reports, 8,* 106–112. https://doi.org/10.1038/s41598-018-32779-3.

Maestrini, B., & Basso, B. (2018b). Predicting spatial patterns of within-field crop yield variability. *Field Crops Research, 219,* 106–112. https://doi.org/10.1016/j.fcr.2018.01.028.

Pebesma, E. J. (2004). Multivariable geostatistics in S: The gstat package. *Computers & Geosciences, 30,* 683–691. https://doi.org/10.1016/j.cageo.2004.03.012.

Philips, D. L., Lee, E. H., Herstrom, A. A., Hogsett, W. E., & Tingey, D. T. (1997). Use of auxiliary data for spatial interpolation of ozone exposure in southeastern forests. *Environmetrics, 8,* 43–61. https://doi.org/10.1002/(sici)1099-095x(199701)8:1%3c43::aid-env237%3e3.0.co;2-g.

R Core Team. (2019). R: A language and environment for statistical computing. Vienna, Austria: R Foundation for Statistical Computing. https://www.R-project.org/

Ross, K., Morris, D., & Johannsen, C. J. (2008). A review of intra-field yield estimation from yield monitor data. *Applied Engineering in Agriculture, 24,* 309–317. https://doi.org/10.13031/2013.24496.

Rouhani, S. (1986). Comparative study of ground-water mapping techniques. *Ground Water, 24*(2), 207–216. https://doi.org/10.1111/j.1745-6584.1986.tb00996.x.

Souza, E. G., Bazzi, C. L., Khosla, R., Uribe-Opazo, M. A., & Reich, R. M. (2016). Interpolation type and data computation of crop yield maps is important for precision crop production. *Journal of Plant Nutrition, 39*(4), 531–538. https://doi.org/10.1080/01904167.2015.1124893.

Sudduth, K. A., & Drummond, S. T. (2007). Yield editor. *Agronomy Journal, 99*(6), 1471–1482. https://doi.org/10.2134/agronj2006.0326.

Sudduth, K. A., Drummond, S. T., & Myers, D. B. (2012). Yield editor 2.0: Software for automated removal of yield map errors. Paper No. 121338243. St. Joseph, MI, USA: ASABE. https://doi.org/10.13031/2013.41893.

Thylén, L., Algerbo, P.A., Giebel, A., Robert, P. C., Rust, R. H., & Larson, W. E. (2000). An expert filter removing erroneous yield data. In Robert, P. C., R. H. Rust, & W. E. Larson (Eds.), *Proceedings of the 5th international conference on precision agriculture and other precision resources management.* Madison, WI, USA: ASA/CSSA/SSSA – CDROM.

USDA. (2019a). United States Department of Agriculture - New York State Agriculture Overview. Retrieved August 19, 2020, from https://www.nass.usda.gov/Quick_Stats/Ag_Overview/stateOverview.php?state=NEW%20YORK.

USDA. (2019b). United States Department of Agriculture - Crop Production 2019 Summary. Retrieved from August 19, 2020, from https://www.nass.usda.gov/Publications/Todays_Reports/reports/cropan20.pdf.

Van Meirvenne, M., Scheldeman, K., Baert, G., & Hofman, G. (1994). Quantification of soil textural fractions of Bas-Zaire using soil map polygons and/or point observations. *Geoderma, 62,* 69–82. https://doi.org/10.1016/0016-7061(94)90028-0.

Vecchia, A. (1988). Estimation and model identification for continuous spatial processes. *Journal of the Royal Statistical Society Series B (Methodological), 50*(2), 297–312. https://doi.org/10.1111/j.2517-6161.1988.tb01729.x.

Vega, A., Córdoba, M., Castro-Franco, M., & Balzarini, M. (2019). Protocol for automating error removal from yield maps. *Precision Agriculture, 20,* 1033–1044. https://doi.org/10.1007/s11119-018-09632-8.

Weber, D., & Englund, E. (1994). Evaluation and comparison of spatial interpolators II. *Mathematical Geology, 26*(5), 589–603. https://doi.org/10.1007/bf02089243.

Wettschereck, D. (1994). A study of distance-based machine learning algorithms. Ph.D thesis, Oregon State University, Corvallis, OR, USA.

Yang, C., Bradford, J., & Wiegand, C. (2001). Airborne multispectral imagery for mapping variable growing conditions and yields of cotton, grain sorghum, and corn. *Transactions of the ASAE, 44*(6), 1983–1994. https://doi.org/10.13031/2013.6997.